Journal of Applied Sciences

ISSN 1812-5654

science alert

ANSInet
an open access publisher
http://ansinet.com

Journal of Applied Sciences 6 (10): 2245-2250, 2006
ISSN 1812-5654
© 2006 Asian Network for Scientific Information

Wheel Attitude Cancellation Thruster Torque of LEO Microsatellite During Orbital Maintenance

[1]A.M. Si Mohammed, [2]M. Benyettou, [1]S. Chouraqui, [3]Y. Hashida and [3]M.N. Sweeting
[1]National Centre of Space Techniques, Division of Space Mechanics,
1 Avenue de la Palestine BP 13 31200-Arzew, Oran, Algeria
[2]Department of Data Processing, Industrial Optimization and Modelling Laboratory,
University of Sciences and Technology of Oran, USTO, BP 1505, El M'Nouar, Oran, Algeria
[3]Surrey Satellite Technology Limited, Surrey GU2 7XH, Guilford, United Kingdom

Abstract: A cold gas propulsion system is used for orbital maintenance on board microsatellite. Cold gas thrusters are the simplest way of achieving thrust. A microsatellite could be a part of the constellation and to maintain a daily coverage, it will be equipped with a propulsion system for an orbit control. A constellation of several microsatellites could be launched and put at the allocate position in the orbit. To do this, the satellites need few months to be in their final position. A propulsion system is used, among other things, to maintain the satellite at its nominal position. The wheels (reaction/momentum) will be used to dump the thruster disturbances caused by misalignment. This study describes the wheel attitude damping thruster disturbances of Low Earth Orbit (LEO) microsatellite for orbit maintenance with the following points: 1) Attitude dynamics, 2) External disturbances, 3) Magnetic wheel control, 4) Simulation results will be presented to evaluate the performance and design objectives.

Key words: Attitude, control, wheel, thruster, microsatellite

INTRODUCTION

Three momentum/reaction wheels are installed in a three-axis configuration to enable full control of the attitude and angular momentum of the satellite. Reaction wheels are essentially torque motors with high-inertia rotors. They can spin in either direction. Roughly speaking one wheel provides for the control of one axis. A minimum of three wheels is needed for full 3-axis control. Momentum wheels are wheels with a nominal spin rate above zero. Their aim is to provide a nearly constant angular momentum. This momentum provides gyroscopic stiffness to two axes, while the motor torque may be controlled to precisely point around the third axis.

In sizing the wheels, it is important to distinguish between cyclic and secular disturbances and between angular momentum storage and torque authority. For three-axis control systems, cyclic torques build up cyclic angular momentum in the reaction wheels, because the wheels are providing compensating torques to counteract these disturbances. We typically size the angular momentum capacity of a reaction wheel (limited by its saturation speed) to handle the cyclic storage during an orbit without the need for frequent momentum dumping. The secular torques and our total storage capacity then define how frequently the angular momentum must be dumped. The torque capability of the wheels usually is determined by slew requirements or the need for control authority above the peak disturbance torque in order for the wheels to maintain the required pointing accuracy (Steyn, 1995):

The wheels are used for the following control functions:

- Cancellation of the disturbance torque caused by the propulsion system during orbit control;
- Full 3-axis pointing and slow slew manoeuvres during imaging;
- Nadir, sun or inertial pointing of the payloads by using angular momentum stiffening;
- Fast spin-up or spin down of the satellite body.

ATTITUDE DYNAMICS

The dynamics of the spacecraft in inertial space is governed by Euler's equations of motion can be expressed as follows in vector form (Chang, 1992)

$$I\dot{\omega}_B^I = N_{GG} + N_D + N_M + N_T - \omega_B^I \times (I\omega_B^I + h) - \dot{h} \quad (1)$$

Corresponding Author: M. Benyettou, Department of Data Processing, Industrial Optimization and Modelling Laboratory, University of Sciences and Technology of Oran, USTO, BP 1505, El M'Nouar, Oran, Algeria
Tel: 213 41 42 0680

Where ω_B^I, I, N_{GG}, N_D, N_M and N_T are, respectively the inertially referenced body angular velocity vector, moment of inertia of spacecraft, gravity-gradient torque vector, applied magnetorquer control firing, unmodelled external disturbance torque vector such as aerodynamic or solar radiation pressure.

The rate of change of the quaternion is given by

$$\dot{q} = \frac{1}{2}\Omega q = \frac{1}{2}\Lambda(q)\omega_B^O \tag{2}$$

Where

$$\Omega = \begin{bmatrix} 0 & \omega_{oz} & -\omega_{oy} & \omega_{ox} \\ -\omega_{oz} & 0 & \omega_{ox} & \omega_{oy} \\ \omega_{oy} & -\omega_{ox} & 0 & \omega_{oz} \\ -\omega_{ox} & -\omega_{oy} & -\omega_{oz} & 0 \end{bmatrix} \tag{3}$$

$$\Lambda(q) = \begin{bmatrix} q_4 & -q_3 & q_2 \\ q_3 & q_4 & -q_1 \\ -q_2 & q_1 & q_4 \\ -q_1 & -q_2 & -q_3 \end{bmatrix} \tag{4}$$

Where, $\omega_B^O = [\omega_{ox}\ \omega_{oy}\ \omega_{oz}]^T$ cbody angular velocity vector referenced to orbital coordinates.

The angular body rates referenced to the orbit coordinates can be obtained from the inertially referenced body rates by using the transformation matrix A:

$$\omega_B^O = \omega_B^I - A\omega_0 \tag{5}$$

The kinematic equations can derived by using a spacecraft referenced angular velocity vector ω_B^R as follows:

$$\begin{aligned} \dot{\theta} &= (\omega_{Rx}\sin\psi + \omega_{Ry}\cos\psi)\sec\phi \\ \dot{\phi} &= \omega_{Rx}\cos\psi - \omega_{Ry}\sin\psi \\ \dot{\psi} &= \omega_{Rz} + (\omega_{Rx}\sin\psi + \omega_{Ry}\cos\psi)\tan\phi \end{aligned} \tag{6}$$

Where $\omega_B^R = \begin{bmatrix} \omega_{Rx} & \omega_{Ry} & \omega_{Rz} \end{bmatrix}^T$ body relative angular velocity in any reference coordinate frame.

EXTERNAL DISTURBANCES
GRAVITY GRADIENT

The gravity gradient disturbance is a torque experienced by a low Earth orbiting spacecraft. This disturbance is created by the unsymmetrical mass distribution of the spacecraft, causing a slight difference in the gravity forces acting on the body. The result is a torque around the spacecraft centre of mass (Hodgard, 1989). The gravity gradient torque is expressed as follows

$$N_{ggx} = 3\omega_o^2 \begin{bmatrix} (I_{zz} - I_{yy})A_{23}A_{33} + I_{yx}A_{13}A_{33} \\ +I_{yz}A_{33}^2 - I_{zx}A_{13}A_{23} - I_{zy}A_{23}^2 \end{bmatrix} \tag{7}$$

$$N_{ggy} = 3\omega_o^2 \begin{bmatrix} (I_{xx} - I_{zz})A_{13}A_{33} - I_{xy}A_{23}A_{33} \\ -I_{xz}A_{33}^2 + I_{zx}A_{13}^2 + I_{zy}A_{13}A_{23} \end{bmatrix} \tag{8}$$

$$N_{ggz} = 3\omega_o^2 \begin{bmatrix} (I_{yy} - I_{xx})A_{13}A_{23} + I_{xy}A_{23}^2 \\ +I_{xz}A_{23}A_{33} - I_{yx}A_{13}^2 - I_{yz}A_{13}A_{33} \end{bmatrix} \tag{9}$$

Where ω_o is orbital angular rate and A_{ij} are the components of A (attitude transformation matrix) that transforms any vector from the referenced orbital to spacecraft body coordinates.

AERODYNAMIC TORQUE

At the low earth orbits where micro satellites operate, the total atmospheric density is not totally negligible. Furthermore, at these orbits the spacecraft's velocity is also very high. From, we can use the following simplified result: Aerodynamic pressure is directly proportional to the air density and the square of the relative air velocity (Wertz, 1992; Shrivastava and Modi, 1983). The major assumption leading to this result is that any surface exposed to the slipstream of the spacecraft, completely absorbs the momentum of the incoming colliding particle. The aerodynamic disturbance torque vector on a spacecraft structure can then be obtained by taking the cross product of the aerodynamic pressure vector on the total projected area and the vector from the center of mass to the center of pressure of the total structure as follows:

$$N_{AERO} = \rho_a V^2 A_p [c_p x \vec{V}] \tag{10}$$

Where

ρ_a : Atmospheric density;
V : Magnitude of spacecraft's velocity vector;
$\vec{V}$: Unit velocity vector;
A_p : Total projected area of spacecraft;
c_p : Vector between center of mass and center of pressure.

The atmospheric density is a strong function of altitude, solar activity and whether the sun is visible or not (orbit day or night). Table 1 list the expected air

Table 1: Typical atmospheric density [kg m^{-3}]

	Perigee (7049 km)	Apogee (7078 km)
Average solar activity	1.24×10^{-14}	6.95×10^{-15}
High solar activity	1.59×10^{-13}	9.41×10^{-14}

density values at orbit day/night during high or average activity for Alsat-1 (first Algerian micro satellite) apogee and perigee altitudes. Theses values where obtained from (Si Mohammed *et al*., 2005a, b).

For a spacecraft structure such as Alsat-1, the major components contributing to the total aerodynamic torque, are the main box-like body, the boom element and the tip mass. Due to the symmetry of the satellite, the effective aerodynamic torque will be in the direction of the non-rotating body Y axis (the axis that defines the pitch angle) (Si Mohammed *et al*., 2005b).

SOLAR RADIATION PRESSURE

Illumination of the sun on a fully absorbtive surface causes a solar pressure of d_0/c on the surface normal, where d_0 = 1358 Wm^{-2} (the average solar radiation constant) and c is the velocity of light (3×10^8 ms^{-1}). For general surfaces more complicated, (Wertz, 1992). It is normally a function of the absorption, specular and diffuse reflection coefficients.

The worst case scenario of a maximum incidence angle of the solar radiation on fully absorbtive (black body) surfaces, where

$$N_{SOLAR} = 1.74 \times 10^{-7}\,\text{Nm} \tag{11}$$

The worst-case solar radiation disturbance torque is therefore is the same order to the maximum aerodynamic disturbance torque and then we add it and its influence cannot be ignored.

EARTH'S MAGNETIC FIELD

The Earth's magnetic field can be characterized by a magnetic dipole such as that produced by a current loop or a sphere of uniform magnetization. The magnetic field can more accurately be expressed mathematically by a spherical harmonic model, the so-called IGRF (International Geomagnetic Reference Field) model (Wertz, 1992). Due to secular drift and magnitude decrease of the geomagnetic field, the coefficients of the IGRF model are updated every 5 years and supplied with secular variation terms. For the purpose of simulation, a first order dipole model will be used to represent the geomagnetic field vector. This dipole vector can be expressed as follows:

$$B = \nabla\left[\frac{\vec{R}^{T}M_e}{R_s^3}\right] = \frac{M_e}{R_s^3}\left[1 - 3\vec{R}\vec{R}^{T}\right] \tag{12}$$

Where

∇ : Vector gradient operator;
R_S : Geocentric position vector length;
$\vec{R}$: Unit geocentric position vector;
M_e : Vector geomagnetic strength of dipole;
1 : Identity matrix.

MAGNETIC WHEEL CONTROL

Any reaction wheel 3-axis stabilised satellite must employ a momentum management algorithm to restrict the wheel momentum within allowable limits. Momentum build-up naturally occurs due to the influence of external disturbance torques, for example, the torques due to passive gravity gradient, aerodynamic and solar forces and active control torques from thrusters and magnetorquers (MT). These disturbances to the body of an attitude-controlled satellite cause an accumulation of momentum on the reaction wheels. The added momentum may cause saturation of the reaction wheel speed. Moreover, the existence of large angular momentum in the satellite causes control difficulties when attitude controllers are implemented, because the momentum provides the satellite with unwanted gyroscopic stability. Therefore, the management of three-axis reaction wheel momentum is required in order to counteract the influence of persistent external disturbance torques. A cheap and effective means of active unloading of this momentum is making use of magnetorquers, to force the wheel speed back to nearly zero speed.

Magnetorquers generate magnetic dipole moments whose interactions with the Earth's magnetic field produce the torques necessary to remove the excess momentum. The magnetic torque vector can be expressed as the cross product of the magnetic dipole moment M of the magnetic coils with the geomagnetic field strength B in the body frame (Hodgart and Ong, 1994; Martel *et al*., 1988):

$$N_M = M \times B = \Psi(t)M \tag{13}$$

Where M is the magnetic dipole control moment vector;

$$\Psi(t) = \begin{bmatrix} 0 & B_z(t) & -B_y(t) \\ -B_z(t) & 0 & B_x(t) \\ B_y(t) & -B_x(t) & 0 \end{bmatrix} \tag{14}$$

The magnetic field B in the body coordinates can be modelled by:

$$B = Ab_0 \quad (15)$$

Where B_0 is the geomagnetic field vector in the local orbital coordinates from an IGRF model.

The cross-product law algorithm was proposed to dump the extra momentum from the reaction wheel and can be written as Chang *et al.* (1992) and Si Mohammed *et al.* (2004).

$$M = \frac{k_m(h \times B)}{\|B\|} \quad (16)$$

Where k_m is a scalar gain.

SIMULATION RESULTS

The results presented in this paper were obtained with a simulator that implements the dynamics and kinematics of the satellite using C code, MATLAB and SIMULINK. The data in Table 2 to 6 are an example of the initial values of simulations for Low Earth Orbit satellite.

Table 2: Orbit

Inclination [degree]	98
Altitude [km]	860

Table 3: Initial State Vector for the Simulator

Initial Roll angle [degree]	3.0
Initial Pitch angle [degree]	0.0
Initial Yaw angle [degree]	0.0
Initial ω^I_{ox} [degree/second]	0.0
Initial ω^I_{oy} [degree/second]	$-2\pi/6000$
Initial ω^I_{oz} [degree/second]	0.6

Table 4: Measurement Error Variance

Sun sensor measurement error	
Variance in X/Y/Z axis [degree]^2	$(0.1)^2$
Magnetometer measurement error	
Variance in X/Y/Z axis [microTesla]^2	$(0.3)^2$

Table 5: Inertial tensor

I_{xx} [kg m^2]	153.0
I_{xy} [kg m^2]	0.0
I_{xz} [kg m^2]	0.0
I_{yx} [kg m^2]	-0.25
I_{yy} [kg m^2]	153.0
I_{yz} [kg m^2]	0.0005
I_{zx} [kg m^2]	0.1
I_{zy} [kg m^2]	0.0
I_{zz} [kg m^2]	5.0

Table 6: Miscellaneous

Integration step [second]	1
Sampling time [second]	10

Figure 1-4 present the attitude magnetorquer plus Z wheel yaw phase control damping of thruster disturbances for multiple firings of 30 sec.

We assume that the thruster is in the X-axis with the following torque Nx = 0.000005 Nm, Ny = 0.0015 Nm, Nz = 0.0015 Nm. The firing time of the thruster is 30 sec at 40000 and 30 sec at 80000 sec. For 30 sec firing the yaw angle is achieving a disturbance angle of 80 degrees and the roll angle is achieving a disturbance angle of 5 degrees and the pitch angle are achieving a disturbance angle of 2 degrees. Damping of the attitude disturbances is achieved within 1.5 orbits.

The total accumulated on time of magnetorquer is approximately 18920 sec during an active control window of 20 orbits. This gives an average magnetorquer power drain of 0.22 Watt.

Figure 5-8 present the attitude magnetorquer plus Y wheel control damping of thruster disturbances for multiple firings of 30 sec.

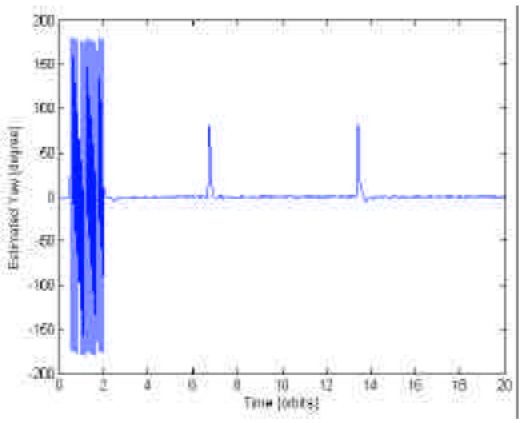

Fig. 1: Yaw Attitude during MT plus Z wheel yaw phase control damping of thruster disturbances

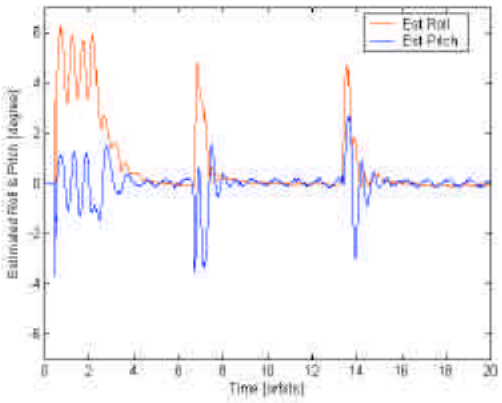

Fig. 2: Roll and Pitch Attitude during MT plus Z wheel yaw phase control damping of thruster disturbances

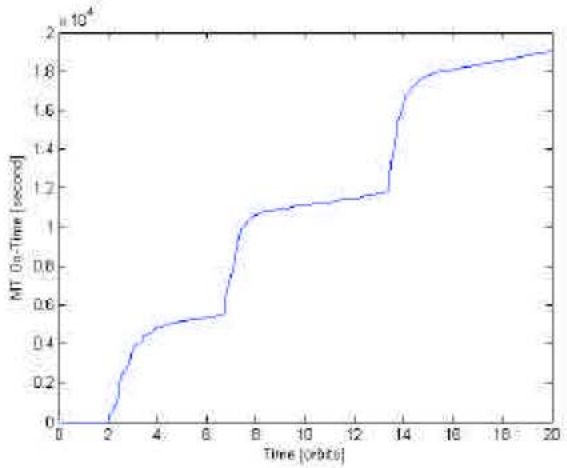

Fig. 3: Magnetorquer activity during MT plus Z wheel yaw phase control damping of thruster disturbances

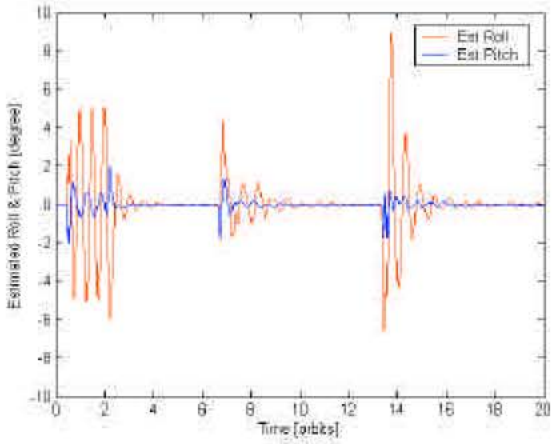

Fig. 6: Roll and Pitch Attitude during MT plus Y wheel control damping of thruster disturbances

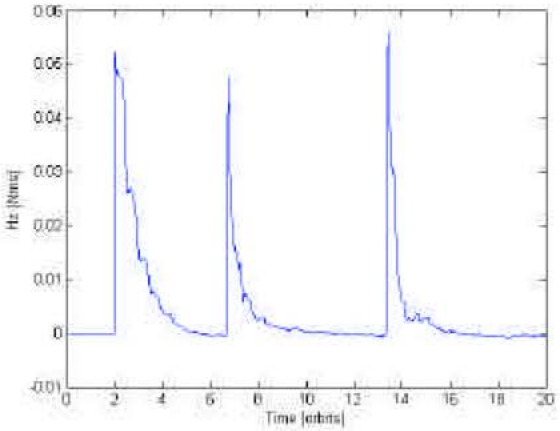

Fig. 4: Z wheel momentum during MT plus Z wheel yaw phase control damping of thruster disturbances

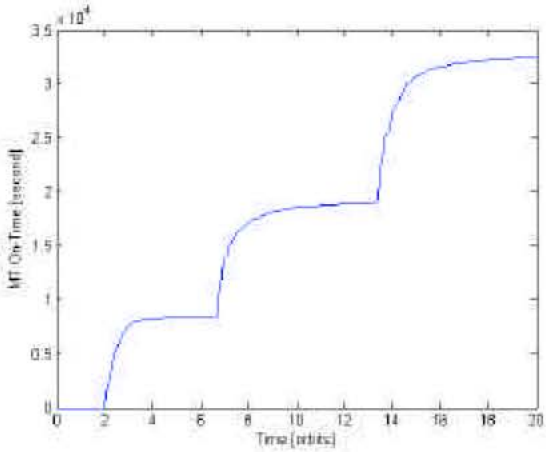

Fig. 7: Magnetorquer activity during MT plus Y wheel control damping of thruster disturbances

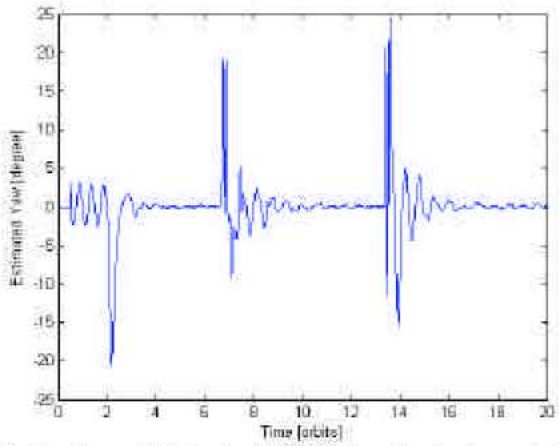

Fig. 5: Yaw Attitude during MT plus Y wheel control damping of thruster disturbances

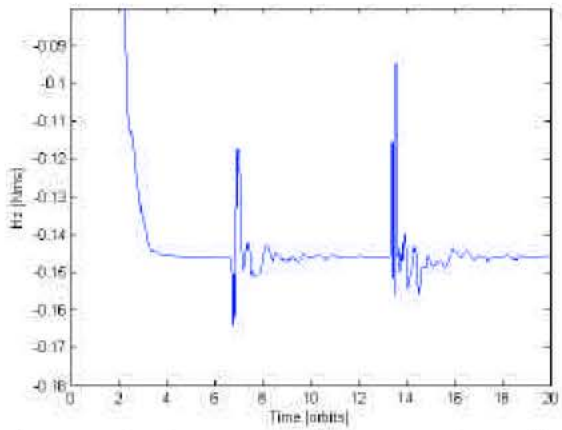

Fig. 8: Y wheel momentum during MT plus Y wheel control damping of thruster disturbances

We assume that the thruster is in the X-axis with the following torque Nx = 0.000005 Nm, Ny = 0.0015 Nm, Nz = 0.0015 Nm. The firing time of the thruster is 30 sec at 40000 and 30 sec at 80000 sec. For 30 sec firing the yaw angle is achieving a disturbance angle of 25 degrees and the roll angle is achieving a disturbance angle of 10 degrees and the pitch angle are achieving a disturbance angle of 8 degrees. Damping of the attitude disturbances is achieved within 5 orbits.

The total accumulated on time of magnetorquer is approximately 32550 sec during an active control window of 18 orbits. This gives an average magnetorquer power drain of 0.9 Watt.

CONCLUSIONS

Misalignment of the thrust vector to the center of mass of the satellite can cause significant disturbances to the attitude.

For magnetorquer plus Z wheel yaw phase control damping of thruster disturbances, the yaw angle is achieving a disturbance angle of 80 degrees and the roll angle is achieving a disturbance angle of 5 degrees and the pitch angle are achieving a disturbance angle of 2 degrees. Damping of the attitude disturbances is achieved within 1.5 orbits.

For magnetorquer plus Y wheel control damping of thruster disturbances the yaw angle is achieving a disturbance angle of 25 degrees and the roll angle is achieving a disturbance angle of 10 degrees and the pitch angle are achieving a disturbance angle of 8 degrees. Damping of the attitude disturbances is achieved within 5 orbits.

REFERENCES

Chang, D.H., 1992. Magnetic and Momentum Bias Attitude Control Design for the HETE Small Satellite. Communications of the 6th AIAA/USU Conference on Small Satellites, Utah State University, USA.

Hodgart, M.S., 1989. Gravity Gradient and Magnetorquing Attitude Control for Low Cost Low Earth Orbit Satellites- the UoSAT Experience. Ph.D. Thesis, University of Surrey, UK.

Hodgart, M.S. and W.T. Ong, 1994. Attitude Determination and Control for Low Earth Orbit Microsatellite. Proceedings IEEE/SAIEE 1994 Symposium on Small Satellites and Control, University of Stellenbosch.

Martel, F., P.K. Pal and M. Psiaki, 1988. Active Magnetic Control System for Gravity Gradient Stabilized Spacecraft. Proceedings of the 2nd AIAA/USU Conference on Small Satellites. Utah State University, USA., pp: 230-238.

Shrivastava, S.K. and V.J. Modi, 1983. Satellite attitude dynamics and control in the presence of environmental torques-a brief survey. J. Guidance, Control and Dynamics, 6: 923-936.

Si Mohammed, A.M, M.N. Sweeting and J.R. Cooksley, 2004. Modelling and Simulation of Magnetic Control and its Application on Alsat-1 First Algerian Microsatellite. Proceeding 18th European Simulation Multiconference, Networked Simulations and Simulated Networks, SCS-The Society for Modeling and Simulation International, 13-16 June, Magdeburg, Germany.

Si Mohammed, A.M., M. Benyettou, M.N. Sweeting and J.R. Cooksley, 2005a. Imaging Mode Results of the Alsat-1 First Algerian Microsatellite in Orbit. Proceeding IEEE Recent Advances in Space Technologies, RAST 2005, 9-11 June, Istumbul, Turkey, pp: 622-628.

Si Mohammed, A.M., M. Benyettou, M.N. Sweeting and J.R. Cooksley, 2005b. Full Attitude Determination Specification-Small Libration Version-of the Alsat-1 First Algerian Microsatellite in Orbit. Proceeding IEEE Recent Advances in Space Technologies. RAST 2005, 9-11 June, Istumbul, Turkey, pp: 530-535.

Steyn, W.H., 1995. A Multi-Mode Attitude Determination and Control System for Small Satellite. Ph. D. Thesis (Engineering), University of Stellenbosch.

Wertz, J.R., 1992. Spacecraft Attitude Determination and Control. D. Reidel Publishing Company, Dordrecht, Nederland.